DALTON
PERSPECTIVE

Negative thermal expansion materials†

John S. O. Evans

Department of Chemistry, University of Durham, Science Laboratories, South Road, Durham, UK DH1 3LE. E-mail: john.evans@durham.ac.uk

Received 28th May 1999, Accepted 7th July 1999

The vast majority of materials have a positive coefficient of thermal expansion and their volume increases on heating. There has been considerable recent interest in materials which display the unusual property of contracting in volume on heating; *i.e.* those with a negative coefficient of thermal expansion. This Perspective gives an overview of some of the physical phenomena that can give rise to this unusual effect. Recent insights into negative thermal expansion materials and some of their unusual structural properties are discussed.

1 Introduction

It is well known that the vast majority of materials expand on heating—they have a positive coefficient of thermal expansion. At the simplest level this phenomenon can be traced back to the asymmetric shape of a typical interatomic potential well (Fig. 1). For a simple diatomic molecule, the gradual population of higher energy vibrational levels will lead to an increase in bond distance with increasing temperature.[1,2] For more complex systems, such as most inorganic solids, one must consider the population of the entire phonon density of states as a function of temperature, but the simple picture remains generally true: the population of higher energy vibrational modes tends to give rise to thermal expansion. There are, however, certain categories of materials for which the underlying thermal expansion of chemical bonds may become dominated by other factors which tend to lead to a contraction in volume. Such materials can, in certain temperature ranges, show the more unusual property of negative thermal expansion (NTE).

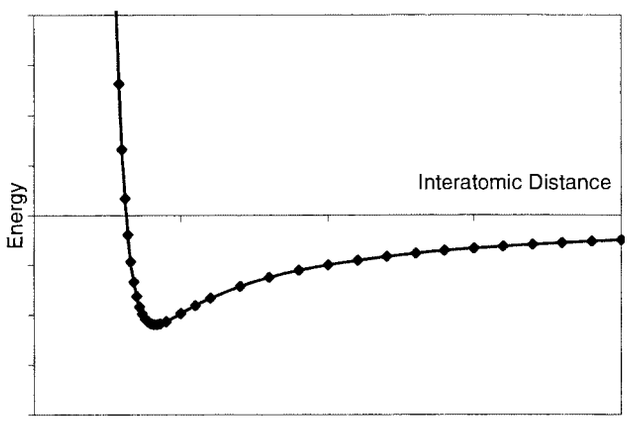

Fig. 1 Potential energy curve for a typical chemical bond.

There are a number of important potential applications for substances with a negative coefficient of thermal expansion. Perhaps the most obvious is in composite materials where the overall expansion coefficient of a body can be precisely tailored to a specific positive, negative or even zero value. Zero expansion composites can be employed, for example, in high precision optical mirrors, where thin metallic layers are coated on a substrate; the use of a zero expansion substrate leads to a mirror whose optical properties do not degrade as temperature is varied. Controlled expansion composites are also likely to find applications in fibre optic systems and as packaging materials for refractive index gratings, where negative thermal expansion materials can be used to compensate for changes in the refractive index and dimensions of glass fibres as temperature changes, leading to more precise control of reflected wavelength. Low expansion ceramics are also of use for their resistance to thermal shock; Pyrex© glass and oven-to-table

Dr John S. O. Evans was born in Gloucestershire in 1968. He obtained his first degree from Keble College, Oxford in 1990 and his D.Phil. from Oxford in 1993, under the supervision of Professor Dermot O'Hare. He then spent two years as a post doctoral research assistant with Professor Art W. Sleight at Oregon State University. After this period he returned to Oxford to take up an 1851 fellowship and in 1997 became a lecturer at Balliol College. He was the recipient of the RSC Meldola Medal in 1997, and in 1998 was appointed to his current position as a lecturer in inorganic chemistry at the University of Durham. His research interests encompass a range of topics in solid state chemistry.

John S. O. Evans

† *Electronic supplementary information (ESI) available*: oxygen migration in ZrW_2O_8; high pressure phase transition in ZrW_2O_8; low energy arrangements of polyhedra within the unit cell of ZrV_2O_7; structure of ZrW_2O_8; the rigid unit mode of a 2-D perovskite; the potential structural flexibility of ZrW_2O_8 as a side-on view and also viewed down the threefold axis. See http://www.rsc.org/suppdata/dt/1999/3317/, otherwise available at http://www.dur.ac.uk/~dch0jse/.

Table 1 Thermal expansion coefficients of common materials. α_l values are, in general, temperature dependent. Values are quoted at a specific temperature or over a given temperature range

Material	α_l ($\times 10^{-6}$)/K^{-1}	T/K	Ref.
Si	+2.45	373–223	21
Cu	+16.64	293	22
Ice	−5	45	23
Ice	0	63	23
Ice	+55	250	23
NaCl	+39.6	293	22
Alsint 99.7% Al_2O_3	+7.8		24
α-Quartz	42	223–373	5
β-Quartz	0	575–1000	5
Fused Quartz	0.5	300	22
Invar	0.07	278–303	20
$NaTi_2(PO_4)_3$	+4.2	300–1000	18
$NbZr(PO_4)_3$	−2.3	300–1000	18
ZrW_2O_8	−9.1	0–300	25
ZrV_2O_7	−7.1	400–500	26
$Sc_2(WO_4)_3$	−2.2	10–450	27

cookware being perhaps the best known examples of this application. Materials with a coefficient of thermal expansion matched to that of another material are also of importance in electronic and biomedical applications. There are obvious advantages in tailoring the thermal expansion properties of printed circuit boards and heat sinks in the electronics industry to match those of silicon; dental fillings need to have their expansion coefficients matched to those of teeth. Finally, materials that display negative thermal expansion (and particularly those that continue to do so down to very low temperatures (see below)) could find uses in low temperature sensing applications.

In this Perspective I will attempt to describe some of the phenomena which can give rise to the occurrence of negative thermal expansion, then concentrate on three families of materials which have aroused considerable interest over the past few years for the magnitude and temperature range over which they display this unusual phenomenon—the ZrW_2O_8, ZrP_2O_7 and $Sc_2(WO_4)_3$ families. In doing so it will become apparent that these structurally fascinating materials display a wealth of interesting properties. The majority of the science reviewed here will be from literature published in the last 3 years. There are a number of excellent reviews covering earlier discoveries, as well as a detailed compendium of data gathered by Taylor in the 1980's and early 1990's covering thermal expansion data of a range of oxides.[3–20] Throughout the articles, coefficients of thermal expansion will be quoted as $\alpha_l = (l_T - l_0)/l_0(T - T_0)$ or $\alpha_V = (V_T - V_0)/V_0(T - T_0)$; for a cubic material $\alpha_l = 1/3\alpha_V$. Values of α for typical "normal" materials, some familiar commercially available materials, and some of the more unusual materials described in this article are given in Table 1.

2 Origins of negative thermal expansion

2.1 Phase transitions

As discussed above, in order for a material to display negative thermal expansion there must normally be a structural phenomenon which outweighs the usual tendency of bonds to expand with increasing temperature. There are, however, rare circumstances in which average bond distances in solids can in fact decrease, at least over a narrow temperature range.

Ideas of bond valence originating from the work of Pauling and developed extensively by workers such as Brown and O'Keeffe[28,29] have shown that the contribution to the overall valence sum from a given bond can be well approximated by the expression $v = \exp[(r_0 - r)/0.37]$ where r_0 is a constant for a given E–X combination of elements. This leads to bond strength–bond length relationships of the form shown in

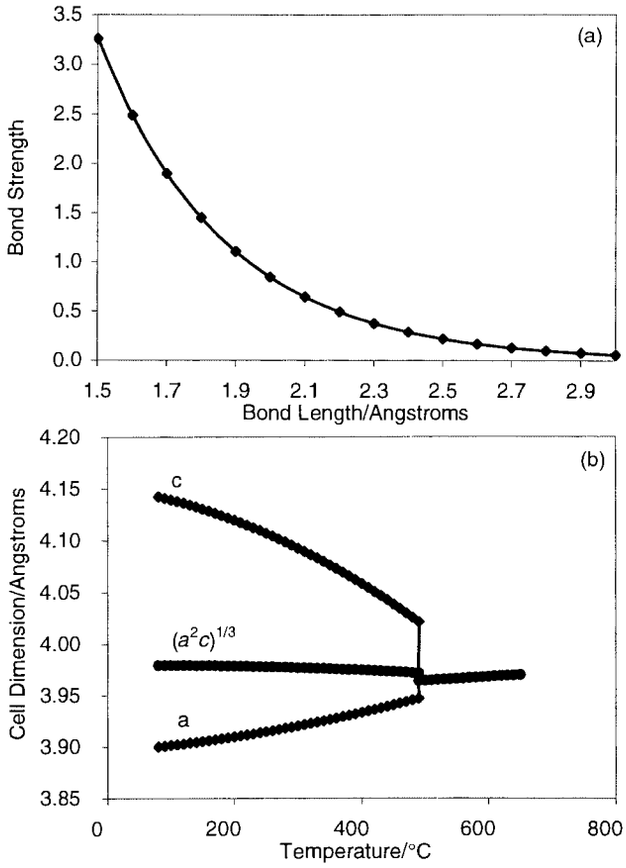

Fig. 2 (a) The form of a typical bond length–bond strength plot. (b) Cell parameters of $PbTiO_3$ as it approaches its tetragonal–cubic phase transition.

Fig. 2(a). From the shape of this curve one can appreciate that the bond length r in, for example, an undistorted MO_6 octahedron will always be shorter than the average bond distance in a distorted octahedron with, for example, 3 short and 3 long bonds. Shannon emphasised the importance of such effects in his 1976 paper on ionic radii.[30]

An example of this effect can be seen in the temperature dependence of the unit cell parameters of $PbTiO_3$ as it approaches its ferroelectric–paraelectric phase transition at 490 °C [Fig. 2(b)].[31] $PbTiO_3$ contains highly distorted Ti octahedra; at room temperature the Ti–O bond lengths are 1.766, 4 × 1.979 and 2.390 Å.[32] On warming these octahedra regularise and the average Ti–O bond length decreases from 2.012 to 1.983 Å (this represents a bond length expansion coefficient of $\alpha_l = -3 \times 10^{-5}$ K^{-1}). This effect presumably contributes to the marked decrease in cell volume as temperature is increased. From 30–400 °C the coefficient of thermal expansion is $\alpha_l = -3.3 \times 10^{-6}$ K^{-1} (value based on $(a^2c)^{1/3}$ as a representative length and the regression analysis figures quoted by Taylor).[8] Agrawal and coworkers have examined the expansion properties of a range of solid solutions of $PbTiO_3$ and related perovskitic materials.[33,34]

2.2 Phonons

In the opening paragraph of this article I described how vibrational modes will, in general, lead to an increase in interatomic distances and hence positive thermal expansion. However, it was first pointed out in the 1950's[35,36] that transverse vibrational modes can lead to the opposite effect and negative thermal expansion.[3] Consideration of the schematic of Fig. 3 shows that for a two-coordinate bridging atom a longitudinal vibration (*e.g.* along an M–O–M bond) will lead to an expansion of the M–M distance. During a transverse vibration, however, if the M–O distance remains essentially unchanged, the M–M distance will decrease. This argument can be put on a

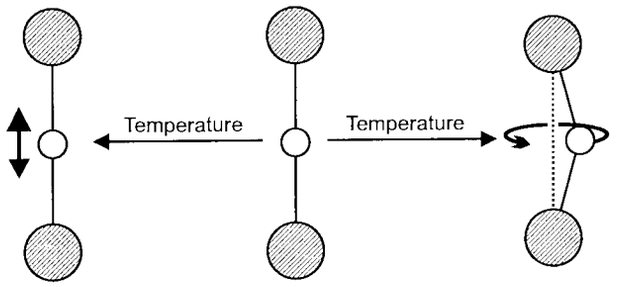

Fig. 3 Schematic representation of the effect of different types of vibrational mode on thermal expansion. Transverse "guitar string" vibrations tend to lead to negative thermal expansion.

more formal basis by considering the relationships between phonons and thermal expansion that were established by Gruneisen in the 1920's.[37] The Gruneisen relationship relates the thermal expansion of a material ($a_V = (1/V)(\partial V/\partial T)_P$) to its volume ($V$), specific heat at constant volume (C_V) and isothermal compressibility ($K = -(1/V)(\partial V/\partial P)_T$).

$$a = \frac{\gamma C_V K}{V} \qquad (1)$$

The Gruneisen parameter, γ, is typically in the range of 1 to 3 and reflects the anharmonicity of a typical crystal potential in that $\gamma = -\mathrm{d}(\ln\ \nu)/\mathrm{d}(\ln\ V)$.Thus vibrational modes whose frequency, ν, decreases (or "softens") as the volume of the material decreases will have a negative Gruneisen parameter and from eqn. (1) will tend to give a negative contribution to the overall thermal expansion. This can be most readily understood by using the "guitar string" analogy of Fig. 3. If one plucks a guitar string (*i.e.* excites a transverse vibrational mode—one which leads to negative thermal expansion) and subsequently stretches the string, the note will move to higher frequency. This is thus the type of vibration which tends to cause negative thermal expansion. To understand the thermal expansion of complex materials one must consider the population of all vibrational modes at a given temperature *i.e.* $\gamma_{av} = \Sigma c_i\gamma_i/\Sigma c_i$, where c_i weights the contribution of a mode to the overall specific heat, C_V. In general, transverse modes are of lower energy than longitudinal modes and are preferentially excited at low temperature. They may thus dominate the overall Gruneisen parameter at low temperatures leading to negative thermal expansion.

The population of low energy transverse modes is the origin of negative thermal expansion at very low temperatures in a number of materials. Rubidium halides with the rock salt structure, for example, show negative thermal expansion at temperatures below ≈1/20th of their Debye temperature ($\theta_D = h\nu_D/k$ where ν_D, the Debye frequency, is a measure of the temperature above which most vibrational modes of a crystal are fully excited—approximately 122 K for RbCl[37]).[3] More open lattices such as the diamond/zinc blende structure will tend to support lower energy transverse vibrational modes and negative thermal expansion has been observed in crystals such as Si, Ga, GaAs, CuCl, $CuFeS_2$ *etc.* Interestingly, correlations can be made between the degree of covalency (rigidity) and the magnitude of the negative thermal expansion. As an example of this general phenomenon, data collected recently on chalcopyrite $CuFeS_2$ which has a zinc blende related structure are shown in Fig. 4(a).[38]

Perhaps the best known everyday example of negative thermal expansion is that of ice. Both the normal hexagonal and cubic forms of ice have a density (0.92 g cm^{-3}) which is lower than that of water. This leads to the well known phenomenon of ice floating on water, a fact essential to the survival of aquatic life. In fact, solid hexagonal ice itself shows negative thermal expansion, albeit only at very low temperatures [Fig. 4(b)].[23] This is again presumably due to low energy transverse vibrational modes with a negative Gruneisen parameter being populated at low temperature.[23,39,40] Tanaka[39] has described the relative importance of different vibrational modes to the overall thermal expansion at different temperatures. He describes a family of low energy (<50 cm^{-1}) modes corresponding to bending motions of 3 water molecules as being largely responsible for the negative thermal expansion at low temperatures.

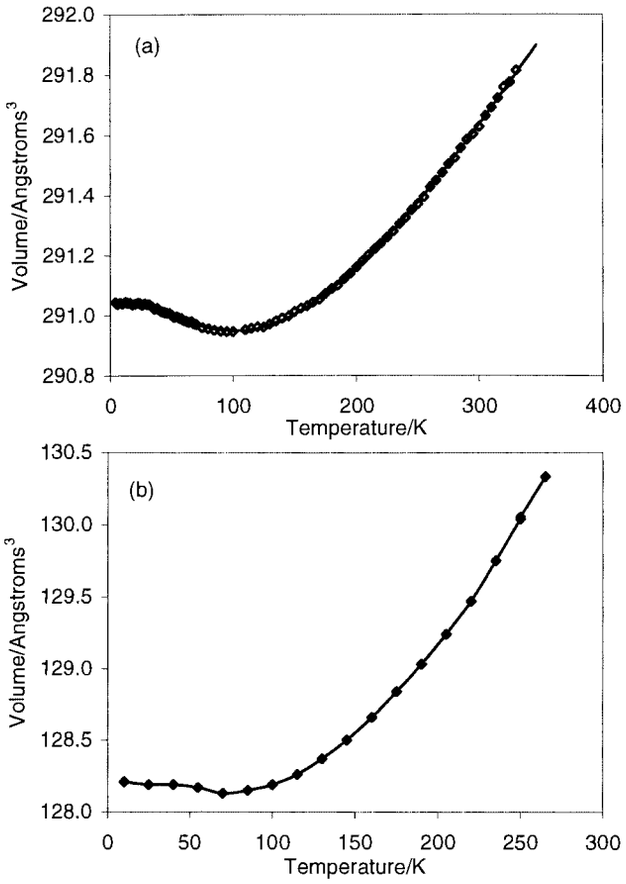

Fig. 4 Thermal expansion curves of (a) $CuFeS_2$ and (b) ice using the data of Knight[38] and Rottger.[23] The solid line in (a) represents a fit to a simple 2-Debye type model. At low temperatures population of modes with a negative Gruneisen parameter leads to negative thermal expansion. At higher temperatures modes with a positive Gruneisen parameter dominate.

2.3 Magnetic transitions

Magnetostrictive phenomena in the region of magnetic phase changes can also give rise to materials with low thermal expansion. For materials with a significant magnetoelastic coupling the "normal" phonon driven positive thermal expansion can be compensated by a large contraction driven by changes in the magnetic structure. This is the case for alloys such as "Invar", $Fe_{0.65}Ni_{0.35}$, and transition metals such as Cr and α-Mn. Correctly processed, Invar has been quoted as having a thermal expansion coefficient of 0.02×10^{-6} K^{-1}, though over a restricted temperature range.[41,42] Materials such as Lu_2Fe_{17} and Y_2Fe_{17} have also been shown to exhibit negative thermal expansion below approximately 400 K.[43]

2.4 Rigid unit modes

Section 2.2 described how certain vibrational modes can lead to negative thermal expansion at very low temperatures; such effects are unlikely to be of use for most practical applications. It has been known for some time, however, that framework minerals such as β-quartz can show negative thermal expansion

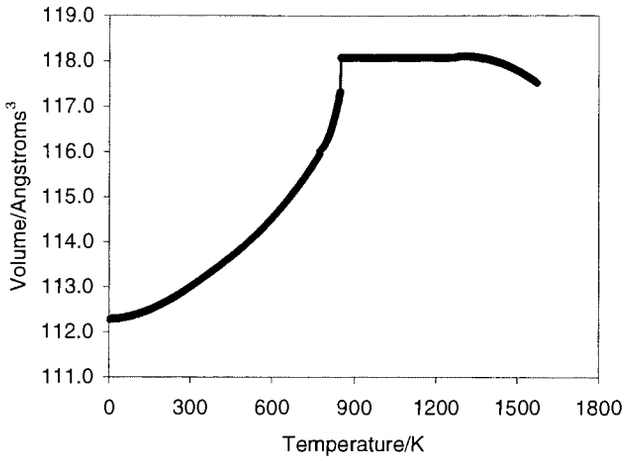

Fig. 5 Thermal expansion of quartz. Plot derived from the data of Taylor.[5] The α ⟹ β phase transition can be seen at 846 K.

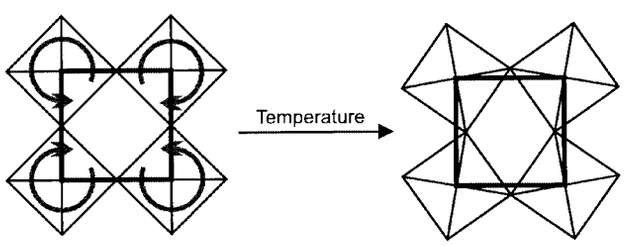

Fig. 6 Schematic representation of how rigid polyhedra in a 2-D perovskite can undergo low energy volume reducing oscillations. An animated version of this figure showing the potential flexibility of the structure is available as ESI.

at high temperatures. Fig. 5 shows the temperature dependence of the unit cell volume of quartz.[5] A model for understanding the origins of such effects in framework materials was initiated by the work of Megaw who described the α to β phase transition in terms of a coupled rotation of relatively rigid corner sharing SiO_4 tetrahedra.[44] These ideas have been extended in recent years, particularly by Dove, Heine and co-workers,[45–53] and a general picture has emerged to describe the occurrence of negative thermal expansion in these materials.

Fig. 6 shows a schematic representation of a framework lattice—a network of corner-sharing squares. This may be thought of as a 2-D slice through the perovskite structure. Individual tetrahedra or octahedra of such a framework are, in general, relatively stiff (strong M–O bonds and relatively short O–O distances preventing distortion of individual polyhedra), but are typically joined by relatively "loose" hinges; M–O–M bending potentials being as much as 100 times weaker than the stiffness of individual polyhedra.

Coupled rotations of these polyhedra [as shown in Fig. 6, and available in an animated version as Electronic Supplementary Information (ESI)] can be envisaged which can occur with no distortion of intrapolyhedral bond distances and angles. These are therefore likely to be low energy distortions, and thus low energy vibrational modes of the structure. Such modes have been termed rigid unit modes (RUM's) or floppy modes by Dove and co-workers.[45–49] The volume reducing tendency of such modes can be readily appreciated from this 2-D example. Following the methodology of Welche *et al.*[50] the area of the unit cell for a tilt angle θ is given by

$$A(\theta) = A_0 \cos^2 \theta \approx A_0(1 - \eta_A \theta^2)$$

where η_A is a geometrical constant specific to a given mode of rotation (which will simply be unity in the case depicted in Fig. 6) and A_0 is the area of the cell for $\theta = 0$. Thus if we consider angular fluctuations of these rigid units around an ideal high symmetry structure, the thermal average of the distortion angle $\langle\theta^2\rangle_T$ will increase with increasing temperature such that the overall unit cell area is given by

$$A(T) = A_0(1 - \eta_A\langle\theta^2\rangle_T)$$

and there is a negative contribution to the overall coefficient of thermal expansion. If one assumes a simple harmonic type motion, and the principle of equipartition of energy, $A(T)$ can be related to the temperature, T, the moment of inertia of the rigid body, I, and the vibrational frequency, ν by

$$A(T) = A_0\left(1 - \eta_A \frac{k_B T}{I\nu^2}\right)$$

where k_B is the Boltzmann constant.

This simple analysis reveals that the population of these modes will lead naturally to negative thermal expansion *via* a "folding up" of the structure and that the lower the vibrational frequency, the greater the impact of that mode on the coefficient of thermal expansion.

Some idea of whether or not a given framework structure will support rigid unit modes can be derived from a simple counting scheme in which one considers the balance between the number of degrees of freedom the structure possesses and its number of constraints. Consider the structure of quartz (an infinite network of corner sharing SiO_4 tetrahedra) as an example: each tetrahedron has 6 degrees of freedom in space—it is free to both rotate and translate in 3 dimensions ($F = 6$); the connectivity of the framework requires, however, that each corner of a tetrahedron be at the same position in space (x, y, z) as the corner of a neighbouring tetrahedron—this represents a total of 12/2 = 6 (as each corner is shared by two tetrahedra) constraints per tetrahedron ($C = 6$). This simple counting scheme shows that the number of degrees of freedom, $N = F - C$, is zero for quartz and its flexibility is marginal. However, this method will always yield the maximum possible number of constraints and in reality many of them are related by symmetry and have thus been "over-counted". Systems with $N = 0$ can be best considered as "potentially flexible" and worthy of more detailed investigation. A more sophisticated method of analysis shows that quartz does indeed possess a large number of rigid unit modes.[47,50,51]

The idea of RUM's has recently been developed within the standard Gruneisen theory of thermal expansion by Heine *et al.* and a detailed description of the thermal expansion properties of β-quartz given.[50] This work describes the importance of the optical RUM's of the type shown in Fig. 6, but also highlights the importance of acoustic modes (many of which are also calculated to have negative Gruneisen parameters) in contributing to negative thermal expansion. In concluding this section, it is worth emphasising that the ideas of RUM's which help explain negative thermal expansion are also important in understanding displacive phase transitions. The same type of modes that lead to NTE at high temperatures are likely to be the soft modes associated with displacive phase transitions at low temperature. Such phase transitions tend to be volume-reducing, as the framework polyhedra undergo coupled rotations. In fact Fig. 5 [and Fig. 14(a), Fig. 15] show thermal expansion plots typical of many materials: quartz shows positive expansion as it approaches a displacive phase transition (polyhedra "unfold") and negative thermal expansion in its high symmetry state. The concepts of rigid unit modes have also given rise to considerable insight into other areas such as solid solutions in mineralogy and the properties of zeolites. Further details are given elsewhere.[45,47,48,52–55]

2.5 Other considerations

Perhaps the best framework in which all of the above phenomena may be described is to consider the change in the internal

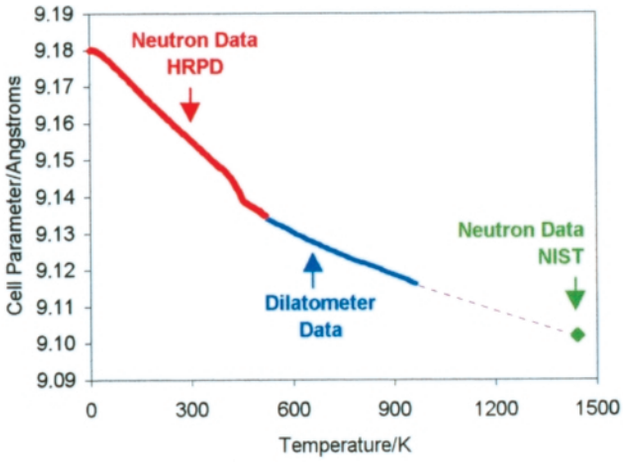

Fig. 7 Thermal expansion behaviour of ZrW_2O_8. Plot shows the cubic unit cell parameter of ZrW_2O_8 from 2 to 1443 K. Data are derived from neutron powder diffraction and dilatometry studies (see text for details). The dilatometer data, where the physical length of a ceramic bar is measured, have been scaled to the cell parameter derived from neutron diffraction data at 298 K. Regions of overlap have been omitted for clarity. ZrW_2O_8 is kinetically stable up to 1050 K, unstable in the dotted region of the curve, and thermodynamically stable at 1443 K.

pressure of a solid caused by heating. This internal pressure will in turn give rise to a volume change. From thermodynamics we can relate the volume coefficient of thermal expansion to the isothermal compressibility K and the internal pressure by

$$\alpha_V = \frac{1}{V}\left(\frac{\partial V}{\partial T}\right)_P = K\left(\frac{\partial P}{\partial T}\right)_V = K\left(\frac{\partial S}{\partial V}\right)_T$$

Thus the sign of the thermal expansion coefficient can be related to the sign of $(\partial S/\partial V)_T$. For normal materials entropy (or the amount of structural disorder) decreases as pressure is increased and volume decreases; all the materials described above, however, show an increase in disorder as volume is reduced.

Finally, it is interesting to note that it is possible to make composites which exhibit negative thermal expansion without relying on any of the above mechanisms. Sigmund and Torquato have shown that it is theoretically possible to produce 3 phase composites which exhibit isotropic negative thermal expansion by engineering a topologically specific combination of two materials with positive thermal expansion (one high one low) and empty space.[56] In theory such composites can be designed such that on heating the bimaterial interfaces of the composite bend in such a way (into the void space) that the overall composite contracts—the material literally folds in on itself.

3 Zirconium tungstate, ZrW_2O_8

3.1 Thermal expansion properties

The material that has stimulated the most interest in the field of negative thermal expansion in recent years is zirconium tungstate, ZrW_2O_8. This simple cubic material was first synthesised and investigated in the 1960's,[57,58] though it is only in the last few years that its structure has been determined, and the extent of its unusual properties realised.[59–61] The reason for the interest in this material is demonstrated most succinctly by Fig. 7. Fig. 7 shows the cubic cell parameter of ZrW_2O_8 as a function of temperature from 2 to 1443 K. Over its entire stability range ZrW_2O_8 exhibits an isotropic negative thermal expansion. The magnitude of this effect is significant, the coefficient of thermal expansion α_l being -9.07×10^{-6} K^{-1} (0–350 K).[25] Zirconium tungstate thus exhibits a contraction which is similar in magnitude to the expansion of conventional ceramic materials and

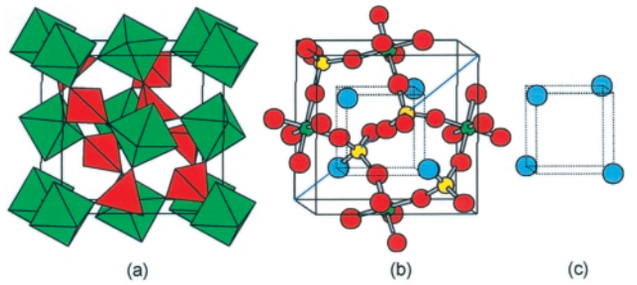

Fig. 8 The structure of cubic ZrW_2O_8. (a) Polyhedral representation: ZrO_6 octahedra (green) share corners with WO_4 tetrahedra (red). (b) Ball and stick representation of a portion of the structure: Zr green, W atoms yellow, two-coordinate O atoms in red. WO_4 tetrahedra lie along the main body diagonal of the cubic unit cell and contain a strictly one-coordinate oxygen (shown in blue). W atoms connected to upper two one-coordinate O's have been omitted for clarity. (c) The 3-D structure of the one-coordinate oxygen atoms. At high temperatures oxygen is disordered over the two available lattice sites. An animated chime representation of the structure is available as ESI.

isotropic in nature—a feature which is of importance in a number of applications, particularly the production of composite materials. Data in Fig. 7 are a combination of neutron powder diffraction (2–520 K; 1443 K), where the unit cell dimensions are determined directly, and dilatometer data, where the physical length of a ceramic block is measured. The only region of the curve where ZrW_2O_8 is thermodynamically stable is the single data point at 1443 K[62] (see below). From 2 to 1050 K, however, quenched cubic ZrW_2O_8 is kinetically stable.

The structure of ZrW_2O_8 is shown in Fig. 8[59–61] (and in chime format as ESI). It may be described as a framework structure containing corner sharing ZrO_6 octahedra and WO_4 tetrahedra. Each octahedron shares each of its 6 corners with a tetrahedron; each tetrahedron, however, shares only 3 of its 4 corners with an octahedron. This arrangement means that there is one oxygen per WO_4 tetrahedron that is formally one-coordinate—a terminal W–O bond. Such an arrangement is extremely unusual in the solid state and is perhaps one of the reasons why ZrW_2O_8 is only metastable at room temperature. Studies by Chang *et al.*[58] show that ZrW_2O_8 is only thermodynamically stable in a narrow temperature range around 1400 K. Once formed, however, it can be quenched to room temperature and is kinetically stable to around 1050 K. At room temperature the relatively open structure of ZrW_2O_8 (density, $\rho = 5.08$ g cm^{-3}) is thermodynamically unstable with respect to the more condensed binaries ZrO_2 ($\rho = 5.83$ g cm^{-3}) and WO_3 ($\rho = 7.19$ g cm^{-3}).

A key feature of the structure of ZrW_2O_8 is the topology of its framework. Using the simple counting scheme described in section 2.4, the number of degrees of freedom for the ZrO_6 and $2WO_4$ polyhedra in the ZrW_2O_8 structure can be defined: there are 18 degrees of freedom (3 polyhedra each having 3 translations and 3 rotations) and 18 constraints (all 6 corners of the ZrO_6 octahedron have (x, y, z) coordinates the same as corners of a WO_4 tetrahedron). The number of degrees of freedom is equal to the number of constraints using this simple counting scheme and ZrW_2O_8 is potentially flexible. The constraints are again, however, not strictly independent and a detailed analysis of ZrW_2O_8 by Pryde *et al.* has revealed that there are a family of rigid and quasi-rigid unit modes (RUM's and QRUM's) present in ZrW_2O_8.[63,64] These authors predicted with their simple model that there would be an unusually high phonon density of states at low energy for ZrW_2O_8. These low energy modes can be expected to give rise to negative thermal expansion. Schematic animations of this type of vibrational mode are given as ESI. Further insight into the vibrational modes responsible for negative thermal expansion comes from the low temperature heat capacity and inelastic neutron scattering experiments reported by Ramirez, Kowach *et al.*[65,66] The measured phonon

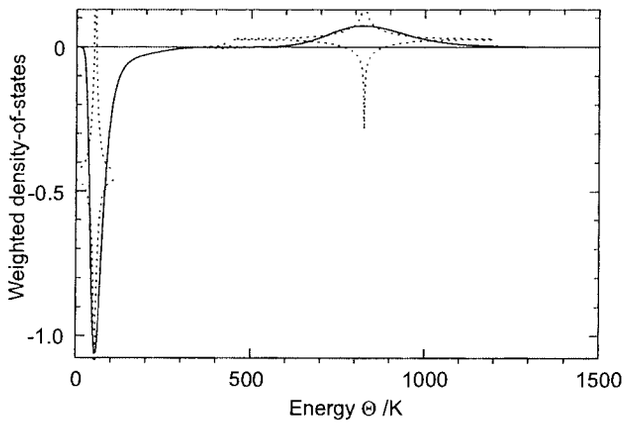

Fig. 9 A maximum entropy reconstruction of the Gruneisen parameter weighted density of states extracted from the cell parameter data of Fig. 7. The negative peak around 55 K (4.7 meV) corresponds to a family of low energy modes which tend to contract the lattice; those centred at 850 K (73 meV) tend to expand the lattice.

density of states shows a low energy family of modes centred around 30 meV and a high energy group centred around 110 meV, though the low energy modes do not extend to zero energy as predicted by the simple RUM model. These data and the unusually high heat capacity of ZrW_2O_8 at low temperature are consistent with a model whereby a family of low energy vibrational modes is responsible for the negative thermal expansion.

Further support for this model has been achieved in a careful examination of the structure of ZrW_2O_8 as a function of temperature. Using neutron powder diffraction techniques and the application of a parametric approach to Rietveld refinement, the structure of ZrW_2O_8 has recently been determined at 260 different temperatures between 2 and 520 K.[25] This work has proved that it is possible to perform a full anisotropic refinement of powder diffraction data despite a data collection time of just 5 minutes. The temperature dependence of the anisotropic displacement parameters can then be analysed to reveal the magnitude of libration of the ZrW_2O_8 polyhedron as a function of temperature and in turn understand the magnitude of the negative thermal expansion.

In fact, the thermal expansion data for a material can be used directly to obtain some information about the phonon density of states.[67] Eqn. (1) shows how the thermal expansion coefficient is related to the heat capacity and compressibility of a material *via* the Gruneisen parameter, γ_i. Fig. 7 contains high precision cell parameter data (2–520 K) collected as a function of temperature using powder diffraction methods. Fig. 9 shows a maximum entropy reconstruction of the Gruneisen parameter weighted phonon density of states based on these cell parameter data and eqn. (1). The maximimum entropy approach means that this is a "least biased" estimate of the true weighted density of states. This curve can be interpreted as showing that there are a family of low energy vibrational modes centred around 4.7 meV (55 K, 39 cm^{-1}) and ranging in energy from 3–8 meV. The frequency of these modes is such that they will be populated at very low temperatures, and their large negative Gruneisen parameter leads to strong thermal contraction from low temperature. At higher energies (≈73 meV, 850 K, 600 cm^{-1}) there are modes which tend to expand the lattice, which can perhaps be interpreted as bond stretches of the individual polyhedra. The essentially zero weighted density of states between 26 and 43 meV (300 and 500 K) suggests that the population of phonons with these thermal energies does not contribute significantly to the overall thermal expansion (α, the slope of Fig. 7, is constant in this range); *i.e.* the weighted Gruneisen parameter for these modes is close to zero.

The unusual vibrational density of states of ZrW_2O_8 is perhaps one reason why the structure is thermodynamically stable with respect to ZrO_2 and WO_3 only around 1400 K. The population of a large family of high amplitude vibrational modes (together with oxygen disorder—see below) presumably provides a significant $-T\Delta S$ contribution to the overall free energy of the material at these high temperatures.

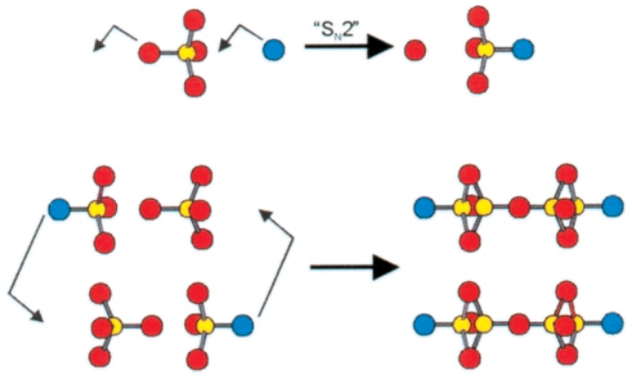

Fig. 10 A schematic representation of the order–disorder phase transition in ZrW_2O_8. An alternative animated view of the phase transition is given as ESI.

3.2 Phase transitions in ZrW_2O_8

It is apparent from Fig. 7 that there is a discontinuity in the measured cell parameter of ZrW_2O_8 at around 450 K. Thermal analysis, dielectric measurements and diffraction data all suggest that this discontinuity is caused by a phase transition from the acentric $P2_13$ structure of Fig. 8 to a disordered centric structure $Pa\bar{3}$.[59] The simplest model for this phase transition is shown schematically in Fig. 10 and available in an animated version as ESI. If one considers a pair of WO_4 tetrahedra pointing along the main body diagonal of Fig. 8(b), then one can see that the terminal oxygen of one WO_4 is perfectly located to "attack" its neighbouring WO_4 tetrahedron in an "S_N2" type fashion. This process can be thought of as creating a "mobile" oxide ion that can then migrate to another set of WO_4 tetrahedra in the structure in a process which effectively reverses the direction in which a pair of tetrahedra point, and leads to a disordered average structure. This process can also be thought of as disordering the terminal oxygen atoms of Fig. 8(b) on a face centred cubic lattice [Fig. 8(c)]. As such, the process is topologically equivalent to an antiferromagnetic to paramagnetic phase transition on the same lattice. The phase transition can be studied by powder diffraction methods as a function of temperature by refining fractional occupancies of the two tetrahedral orientations as a function of temperature. The predicted occupancy data as a function of temperature were taken from calculations by Mark Newman of the Santa Fe Institute based on an Ising model of $100 \times 100 \times 100$ spins. A zero-parameter fit of this model to the refined data is shown in Fig. 11 and supports the topology of the phase transition.[25]

The unusual topology of ZrW_2O_8 is also revealed in its behaviour under applied pressure. Simple geometric modelling studies have shown that under a simulated pressure (artificial reduction of the cell parameter) the individual polyhedral units in ZrW_2O_8 can remain undistorted. As the cubic cell parameter is reduced, the polyhedra can undergo a cooperative system of tilts that leave intrapolyhedral bond distances unaltered and change only relatively soft Zr–O–W bridging angles. It is interesting to note, however, that this treatment predicts an increase in the average bridging bond angles (*i.e.* on average a straightening of framework bonds) on applied pressure.[26] In practice, however, the application of around 2 Kbar of pressure has been shown to drive a phase transition from the cubic α-ZrW_2O_8 structure to an orthorhombic form (γ-ZrW_2O_8).[68,69] The details of this transition are somewhat complicated, but shown schematically in Fig. 12 and in a schematic animation as ESI. A

concerted oxygen migration in ZrW_2O_8 similar to that found at the temperature driven 448 K $\alpha \rightleftharpoons \beta$ phase transition reverses the direction of one in three pairs of WO_4 tetrahedra. Following this process, coupled rotations and distortions of the polyhedra are such that each one-coordinate oxygen enters the coordination sphere of a second W. Thus, at the phase transition the average coordination of each W atom increases but, more crucially, all the one-coordinate oxygen atoms in the structure become two-coordinate.[68–70] γ-ZrW_2O_8 itself shows negative thermal expansion, though an order of magnitude less than cubic α-ZrW_2O_8. This can be related to the increased cross-linking in the structure. γ-ZrW_2O_8 reverts to the cubic α form on heating to around 400 K. From the temperature dependence of the unit cell parameters in this region, one can estimate an activation energy for oxygen migration of around 0.4 ± 0.1 eV.[71] Under higher applied pressure, ZrW_2O_8 has been shown to become amorphous.[72]

Taken together these various observations show that ZrW_2O_8 is an extremely unusual material. In essence cubic ZrW_2O_8 is a metastable material which has been trapped in a local energy minimum. It contains anions in an unusual, unfavourable coordination environment that leads to an unusual topology. The room temperature cubic structure is, however, only one of perhaps many local minima. The application of temperature drives one transition involving oxygen rearrangement; the application of pressure drives a second. Further evidence for yet another local structural minimum comes from the work of Wilkinson *et al.* who have described the preparation of a trigonal form of ZrW_2O_8 structurally analogous to trigonal $ZrMo_2O_8$.[73]

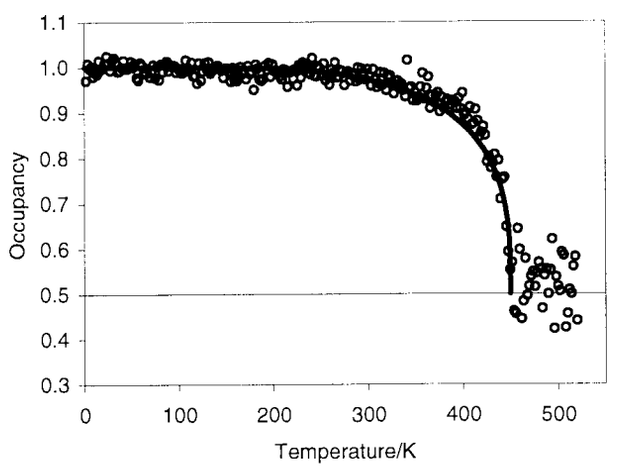

Fig. 11 Fractional occupancy of the low temperature tetrahedral orientation in ZrW_2O_8 as a function of temperature. Solid line represents the fit to a 3-D cubic Ising model (see text).

Related materials in the ZrW_2O_8 family that have been studied include $Zr_{1-x}Hf_xW_2O_8$ materials and the $ZrW_{2-x}Mo_xO_8$ family.[59,74,75] All show isotropic negative thermal expansion. The $x = 1$ and $x = 2$ members of the $ZrW_{2-x}Mo_xO_8$ family have structures at room temperature and below which are analogous to high temperature β-ZrW_2O_8, and contain oxygen disordered over two lattice sites. Work on these compounds is ongoing.

4 AM_2O_7 Materials

The AM_2O_7 (*e.g.* A = Ti, Zr, Hf, Sn; M = P, V) phases are structurally closely related to ZrW_2O_8 and form a second family of cubic materials which display isotropic negative thermal expansion under certain conditions.[76–78] The relationship between the two families can be most readily understood by formally replacing the two unlinked WO_4 tetrahedra of Figs. 8 and 10 by an M_2O_7 group containing two corner linked tetrahedra. AM_2O_7 materials might thus be expected to have a simple cubic structure ($Pa\bar{3}$) with a cell dimension close to ZrW_2O_8 (around 8.77 Å for ZrV_2O_7); indeed the structures of ZrP_2O_7 and ZrV_2O_7 were first reported based on such a cell.[79,80] However, several workers later realised that the symmetry of this structure would require unreasonably short V–O–V bridging bond lengths.[81] Such a situation is reminiscent of the unreasonably short Si–O bond lengths required in the ideal high temperature structure of β-cristobalite.[82] The solution to this apparent problem came in the mid-1960's when Völlenke *et al.*[81] realised that the cell edge of many AM_2O_7 phases was actually tripled relative to the simple cell originally reported. Recent work has confirmed this observation for ZrV_2O_7 and the true structure of the material has been determined.[83] The space group of ZrV_2O_7 remains $Pa\bar{3}$, but the true cell edge is $3 \times 8.77 = 26.3$ Å. The phase transition that leads to the tripling of the cell dimension thus preserves the point group, but destroys 26/27 of the translational symmetry elements and 2/3 of the threefold axes. This reduction in symmetry allows four of the six crystallographically unique V_2O_7 groups in the unit cell (which would be constrained by symmetry to have linear V–O–V linkages) to bend away from 180°. Thus the true structure of ZrV_2O_7 can be derived from the ideal structure (see Fig. 13) by a coupled 3-D rotation of relatively undistorted polyhedral units. It is interesting to note that despite this reduction in symmetry,

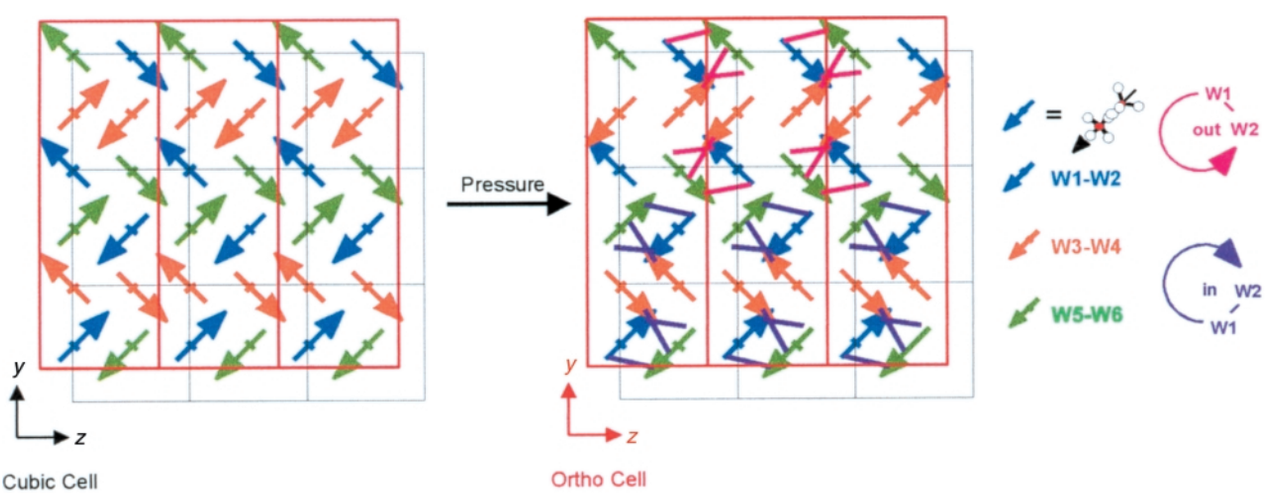

Fig. 12 Schematic representation of the high pressure structure of γ-ZrW_2O_8. 2(WO_4) groups in the low pressure structure (left) are represented in the projection as arrows. Arrows are colour coded according to the symmetry of the high pressure structure. On the application of pressure 1/3 of the groups (orange arrows) change direction. Cross-linking between terminal oxygen atoms of WO_4 groups leads to chains of W centred polyhedra in the high pressure structure. Cubic (α) cell shown in black, orthorhombic (γ) cell shown in red. An animated version of the phase transition is given as ESI.

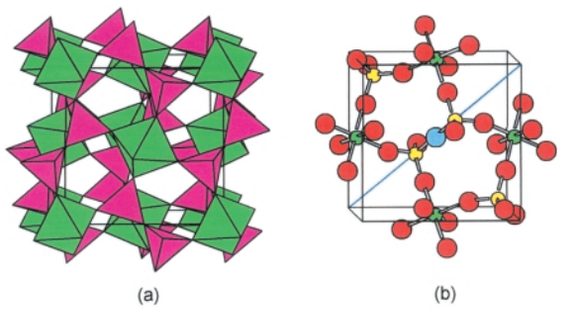

Fig. 13 The ideal simple cubic structure of ZrV_2O_7. (a) ZrO_6 octahedra shown in green share 6 corners with V_2O_7 pyrovanadate groups shown as pink polyhedra. (b) Ball and stick view: Zr green, V yellow, O red. In the ideal high temperature structure all V–O–V bond angles are constrained by symmetry to be 180° and the blue bridging oxygen atom lies on the threefold axis.

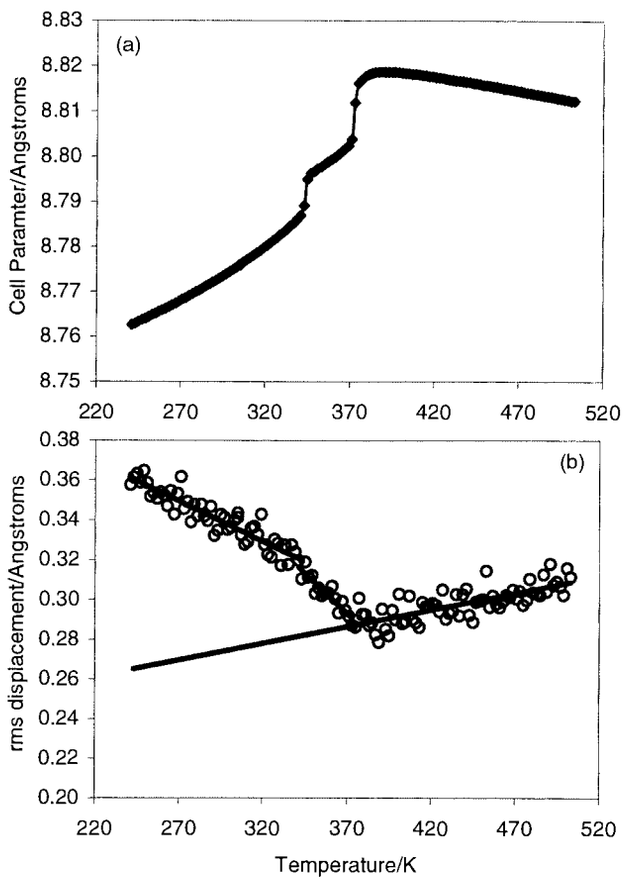

Fig. 14 (a) Cell parameter of ZrV_2O_7 as a function of temperature. Values below 373 K have been divided by 3 for comparison. (b) rms displacement of the V–O–V bridging oxygen atom from its ideal site on the threefold axis as a function of temperature.

some distortion of the ZrO_6 and VO_4 polyhedra is required by the structure topology. Many of the properties of ZrV_2O_7 seem influenced by this necessity for small distortions.

This description of the structure of ZrV_2O_7 can be straightforwardly related to its thermal expansion properties. Fig. 14(a) shows the cubic cell parameter of ZrV_2O_7 as a function of temperature (data below 373 K have been divided by 3 for ease of comparison). As the material is warmed from room temperature its cell volume initially increases. This can be related to an "unfolding" of the polyhedra. At around 345 K the material undergoes a phase transition from its $3a \times 3a \times 3a$ superstructure to an incommensurate structure with cell $\approx 3a \times \approx 3a \times \approx 3a$ (from a modulation wave point of view the modulation vector changes from $\boldsymbol{q} = 1/3\ \langle 110 \rangle^*$ to *e.g.* $\boldsymbol{q} = 0.345\ \langle 110 \rangle^*$). This has been observed by both single crystal X-ray, powder neutron and electron diffraction studies.[83,84] At around 375 K ZrV_2O_7 undergoes a second phase transition to a simple cubic $a \times a \times a$ cell. Above this temperature the material shows strong negative thermal expansion ($\alpha_l = -7.1 \times 10^{-6}$ K^{-1}; 400–500 K). In a simple picture, the material can be thought of as expanding to reach its maximum volume, undergoing a displacive phase transition and then contracting in a manner analogous to the simple picture of Fig. 3. Some feel for the magnitude of this effect and the change in this material from static to dynamic displacement of oxygen positions from their ideal site on the threefold axis, is given by Fig. 14(b).[26] In this figure the rms displacement of the oxygen atom as a function of temperature has been derived from its anisotropic "temperature factor". As the material is warmed from 250 K the temperature factor of the V–O–V bridging oxygens (which are in reality composed of both static and dynamic components) initially decreases as the structure approaches its high symmetry form (V–O–V groups unbend), and then increases as dynamic transverse vibrations of this oxygen increase, resulting in a contraction of the material.

Seo and Whangbo have shown that this picture may be a slight oversimplification (as of course will all models based on 100% rigid units).[85] They point out that a V–O bridging bond length will depend on the V–O–V bridging bond angle. For the analogous P–O–P system, their calculations suggest a reduction in bond length of *ca.* 0.03 Å as the P–O–P bridging bond angle changes from 160° to 180°. This is similar to earlier conclusions on the Si–O–Si units in silicates and can be related to increased multiple bond character (either O lone pair to π* orbitals for P_2O_7 or lone pair to d-orbitals for V_2O_7 groups) in linear groups.[86] There will thus be a tendency for bending vibrations to be coupled to bond stretches, and these effects will have an influence on the overall coefficient of thermal expansion.

The origins of the incommensurate intermediate phase are somewhat unclear. One interesting possible explanation is that the existence of this phase may be related to the observation that more than one low energy arrangement of the polyhedra of ZrV_2O_7 is possible. In the 26.3 Å cubic unit cell there are a total of 108 octahedral and 216 tetrahedral units. Simple DLS modelling studies show that there is more than one way of arranging these units which retains the framework topology and involves only minimal polyhedral distortion (see, for example, the two possible low energy arrangements of polyhedra within the unit cell of ZrV_2O_7 available as ESI). The existence of several alternative low energy structural minima could lead to frustration as the material is warmed.

The thermal expansion properties of ZrP_2O_7 are somewhat similar. ZrP_2O_7 shows a positive coefficient of thermal expansion up to *ca.* 570 K where it undergoes a phase transition to the simple cubic structure, followed by low positive thermal expansion thereafter ($\alpha_l = +5.4 \times 10^{-6}$ K^{-1}; 600–700 K). Sleight and co-workers have shown that the phase transitions, and hence thermal expansion properties, of these materials can be controlled by synthesising solid solutions of the type $ZrV_{2-x}P_xO_7$.[78] For example, phases of the type $ZrV_{0.2}P_{1.8}O_7$ have been shown by dilatometer measurements to display negative thermal expansion from room temperature upwards.

5 $Sc_2(WO_4)_3$ Materials

A third category of materials which has been shown to display negative thermal expansion properties is the scandium tungstate family. The orthorhombic structure of $Sc_2(WO_4)_3$ itself was first described by Abrahams, and again contains corner sharing ScO_6 octahedra and WO_4 tetrahedra.[87] In this material all polyhedral corners are shared. The orthorhombic structure has been shown by neutron powder diffraction to show a contraction in its *a* and *c* axes and an expansion in its *b* axis over a wide temperature range. The relative magnitudes of these effects are such that $Sc_2(WO_4)_3$ shows a marked volume contraction

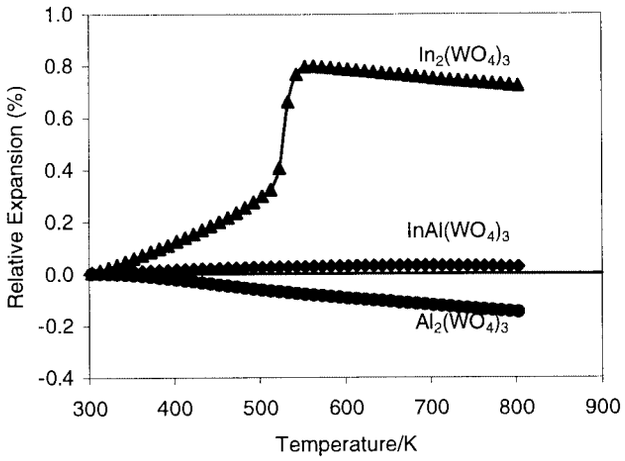

Fig. 15 Relative expansion of three $A_2(WO_4)_3$ materials as a function of temperature. The preparation of solid solutions leads to materials with positive, negative or zero coefficients of thermal expansion.

[$\alpha_V = -6.5 \times 10^{-6}$ K^{-1}; 50–450 K] from 10 to 450 K.[27] This behaviour has again been described in terms of librations of relatively rigid polyhedra in the material.[27]

The $Sc_2(WO_4)_3$ family is of particular interest in that one can substitute a wide range of cations on the Sc site [ranging in size from Al^{3+} (r = 0.675 Å) to Gd^{3+} (r = 1.075 Å)] and both W and Mo on the W site.[88] Isostructural sulfates and selenates are also known. In addition, aliovalent doping leading to phases such as $Zr_2(WO_4)(PO_4)_2$ is also possible.[89] As has been described for several of the framework structures above, some members of the $Sc_2(WO_4)_3$ family of materials undergo a volume reducing phase transition to a monoclinic structure at low temperature.[88,90] The temperature of this phase transition varies from <10 K [$Sc_2(WO_4)_3$ and $Zr_2(WO_4)(PO_4)_2$] to 772 K [$Fe_2(MoO_4)_3$]; in fact T_C can be related directly to the electronegativity of the A site cation. One rationale for this observation is that a significant force driving these volume reducing phase transitions is an increase in the O–O dispersive interactions. The magnitude of such forces will depend on the polarizability of the O atom which in turn depends on the electronegativity of the A site cation. Control of this phase transition can again be achieved by the preparation of solid solutions of the type $AA'(WO_4)_3$, leading to controlled thermal expansion properties. Fig. 15 shows one such example where materials of general formula $Al_{2-x}In_x(WO_4)_3$ have been prepared which, as bulk ceramics, show either positive, negative or close to zero thermal expansion. It should, however, be noted that for anisotropic materials such as these the overall properties of a ceramic bar can differ significantly from changes at the unit cell level. Intergrain effects and microcracking can lead to bulk samples showing enhanced negative thermal expansion. Bars of $Sc_2(WO_4)_3$, for example, can show α_l values as low as -11×10^{-6} K^{-1}.

It has also been shown that the magnitude of the negative coefficient of thermal expansion in these materials can be related to the size of the constituent polyhedra. $Lu_2(WO_4)_3$ [$r(Lu^{3+})$ = 1.001 Å] has been shown to exhibit a bulk contraction of $\alpha_V = -6.8 \times 10^{-6}$ K^{-1}, three times the magnitude of that of $Sc_2(WO_4)_3$ [$r(Sc^{3+})$ = 0.885 Å]; $Y_2(WO_4)_3$ [$r(Y^{3+})$ = 1.040 Å] has $\alpha_V = -7 \times 10^{-6}$ K^{-1}.[91,92]

6 Other materials

There are a number of other classes of framework material that have been shown to display negative thermal expansion. The best known of these is probably the NASICON or NZP family which is based on the $NaZr_2(PO_4)_3$ structure type. These materials are described in much more detail elsewhere.[18,20,93–101] Their anisotropic expansion properties as a function of temperature have been described in terms of a coupled rotation of the constituent building blocks of the structure.[102,103] These properties have in turn been related recently to the presence/absence of cation vacancies in the structure.[104] It is perhaps interesting to note that the one material reported with an intrinsic (*i.e.* at the unit cell rather than bulk ceramic level) negative thermal expansion is the A cation-free $NbZr(PO_4)_3$ ($\alpha_l = -2.3 \times 10^{-6}$ K^{-1}).[18]

Framework materials such as the zeolites have also been shown, both by theoretical predictions and experimental measurements to exhibit negative thermal expansion.[105–109] Again the mechanism is presumably similar to that in other framework materials. That this effect is not restricted to oxides is shown by recent observations of NTE in open structures such as $Zn(CN)_2$ ($\alpha_l = -18 \times 10^{-6}$ K^{-1}), and certain zeotypes.[110]

Acknowledgements

The author would like to acknowledge, *inter alia*, Professor A. W. Sleight of Oregon State University, Dr T. A. Mary, Professor W. I. F. David, Professor J. Jorgensen (and colleagues) and Dr T. Vogt for collaborations in this area and the Royal Commission for the Exhibition of 1851 for a Research Fellowship. I would also like to thank Dr R. M. Ibberson and Dr K. S. Knight for assistance with neutron diffraction measurements, and Dr Knight for supplying the data for Fig. 4. Financial support in terms of access to central facilities from the EPSRC is also gratefully acknowledged.

References

1 R. M. Hazen and C. T. Prewitt, *Am. Mineral.*, 1977, **62**, 309.
2 I. D. Brown, A. Dabkowski and A. McCleary, *Acta Crystallogr., Sect. B*, 1997, **53**, 750.
3 G. K. White, *Contemp. Phys.*, 1993, **34**, 193.
4 D. Taylor, *Br. Ceram. Trans. J.*, 1984, **83**, 92.
5 D. Taylor, *Br. Ceram. Trans. J.*, 1984, **83**, 129.
6 D. Taylor, *Br. Ceram. Trans. J.*, 1984, **83**, 32.
7 D. Taylor, *Br. Ceram. Trans. J.*, 1984, **83**, 5.
8 D. Taylor, *Br. Ceram. Trans. J.*, 1985, **84**, 181.
9 D. Taylor, *Br. Ceram. Trans. J.*, 1985, **84**, 149.
10 D. Taylor, *Br. Ceram. Trans. J.*, 1985, **84**, 121.
11 D. Taylor, *Br. Ceram. Trans. J.*, 1985, **84**, 9.
12 D. Taylor, *Br. Ceram. Trans. J.*, 1986, **85**, 147.
13 D. Taylor, *Br. Ceram. Trans. J.*, 1986, **85**, 111.
14 D. Taylor, *Br. Ceram. Trans. J.*, 1987, **86**, 1.
15 D. Taylor, *Br. Ceram. Trans. J.*, 1988, **87**, 88.
16 D. Taylor, *Br. Ceram. Trans. J.*, 1988, **87**, 39.
17 D. Taylor, *Br. Ceram. Trans. J.*, 1991, **90**, 197.
18 D. Taylor, *Br. Ceram. Trans. J.*, 1991, **90**, 64.
19 D. Taylor, *Br. Ceram. Trans. J.*, 1992, **91**, 217.
20 R. Roy, D. K. Agrawal and H. A. McKinstry, *Annu. Rev. Mater. Sci.*, 1989, **19**, 59.
21 Y. Okada and Y. Tokumaru, *J. Appl. Phys.*, 1984, **56**, 314.
22 T. H. K. Barron, J. G. Collins and G. K. White, *Adv. Phys.*, 1980, **29**, 609.
23 K. Rottger, A. Endriss, J. Ihringer, S. Doyle and W. F. Kuhs, *Acta Crystallogr., Sect. B*, 1994, **50**, 644.
24 Multilab-Ltd., Newcastle upon Tyne, UK, 1999, typical values quoted for commercially available materials.
25 J. S. O. Evans, W. I. F. David and A. W. Sleight, *Acta Crystallogr., Sect. B*, 1999, **55**, 333.
26 J. S. O. Evans, 1999, unpublished work.
27 J. S. O. Evans, T. A. Mary and A. W. Sleight, *J. Solid State Chem.*, 1998, **137**, 148.
28 I. D. Brown and D. Altermatt, *Acta Crystallogr., Sect. B*, 1985, **41**, 244.
29 N. E. Brese and M. O'Keeffe, *Acta Crystallogr., Sect. B*, 1991, **47**, 192.
30 R. D. Shannon, *Acta Crystallogr., Sect. A*, 1976, **32**, 751.
31 G. A. Rossetti, J. P. Cline and A. Navrotsky, *J. Mater. Res.*, 1998, **13**, 3197.
32 A. M. Glazer and S. A. Mabud, *Acta Crystallogr., Sect. B*, 1978, **34**, 1065.
33 D. K. Agrawal, R. Roy and H. A. McKinstry, *Mater. Res. Bull.*, 1987, **22**, 83.
34 D. K. Agrawal, A. Halliyal and J. Belsick, *Mater. Res. Bull.*, 1988, **23**, 159.

35 M. Blackman, *Proc. Phys. Soc.*, 1957, **B70**, 827.
36 T. H. K. Barron, *Ann. Phys.* (*New York*), 1957, **1**, 77.
37 (*a*) E. Gruneisen, *Handb. Phys.*, 1926, **10**, 1; (*b*) S. Elliot, in *The Physics and Chemistry of Solids*, Wiley, Bath, 1998.
38 K. S. Knight, 1999, unpublished work.
39 H. Tanaka, *J. Chem. Phys.*, 1998, **108**, 4887.
40 S. M. Bennington, J. C. Li, M. J. Harris and D. K. Ross, *Physica B*, 1999, **263**, 396.
41 W. F. Schlosser, G. M. Graham and P. P. M. Meincke, *J. Phys. Chem. Solids*, 1971, **32**, 927.
42 S. Chikazumi, *J. Magn. Magn. Mater.*, 1979, **10**, 113.
43 D. Gignoux, D. Givord, F. Givord and R. Lemaire, *J. Magn. Magn. Mater.*, 1979, **10**, 288.
44 H. D. Megaw, in *Crystal Structures a Working Approach*, W. B. Saunders, Philadelphia, 1973.
45 M. T. Dove, *Phase Transitions*, 1997, **61**, 1.
46 M. T. Dove, M. Gambhir, K. D. Hammonds, V. Heine and A. K. A. Pryde, *Phase Transitions*, 1996, **58**, 121.
47 K. D. Hammonds, M. T. Dove, A. P. Giddy, V. Heine and B. Winkler, *Am. Mineral.*, 1996, **81**, 1057.
48 M. T. Dove, V. Heine and K. D. Hammonds, *Miner. Mag.*, 1995, **59**, 629.
49 A. P. Giddy, M. T. Dove, G. S. Pawley and V. Heine, *Acta Crystallogr.*, *Sect. A*, 1993, **49**, 697.
50 P. R. L. Welche, V. Heine and M. T. Dove, *Phys. Chem. Miner.*, 1998, **26**, 63.
51 F. S. Tautz, V. Heine, M. T. Dove and X. J. Chen, *Phys. Chem. Miner.*, 1991, **18**, 326.
52 M. T. Dove, *Am. Mineral.*, 1997, **82**, 213.
53 K. D. Hammonds, V. Heine and M. T. Dove, *Phase Transitions*, 1997, **61**, 155.
54 M. T. Dove, M. J. Harris, A. C. Hannon, J. M. Parker, I. P. Swainson and M. Gambhir, *Phys. Rev. Lett.*, 1997, **78**, 1070.
55 K. D. Hammonds, V. Heine and M. T. Dove, *J. Phys. Chem.*, 1998, **102**, 1759.
56 O. Sigmund and S. Torquato, *J. Mech. Phys. Solids*, 1997, **45**, 1037.
57 J. Graham, A. D. Wadsley, J. H. Weymouth and L. S. Williams, *J. Am. Ceram. Soc.*, 1959, **42**, 570.
58 L. L. Y. Chang, M. G. Scroger and B. Phillips, *J. Am. Ceram. Soc.*, 1967, 211.
59 J. S. O. Evans, T. A. Mary, T. Vogt, M. A. Subramanian and A. W. Sleight, *Chem. Mater.*, 1996, **8**, 2809.
60 T. A. Mary, J. S. O. Evans, T. Vogt and A. W. Sleight, *Science*, 1996, **272**, 90.
61 M. Auray, M. Quarton and M. Leblanc, *Acta Crystallogr.*, *Sect. C*, 1995, **51**, 2210.
62 A. W. Sleight, 1999, unpublished work.
63 A. K. A. Pryde, K. D. Hammonds, M. T. Dove, V. Heine, J. D. Gale and M. C. Warren, *Phase Transitions*, 1997, **61**, 141.
64 A. K. A. Pryde, K. D. Hammonds, M. T. Dove, V. Heine, J. D. Gale and M. C. Warren, *J. Phys. C*, 1996, **8**, 10973.
65 G. Ernst, C. Broholm, G. R. Kowach and A. P. Ramirez, *Nature* (*London*), 1998, **396**, 147.
66 A. P. Ramirez and G. R. Kowach, *Phys. Rev. Lett.*, 1998, **80**, 4903.
67 W. I. F. David, J. S. O. Evans and A. W. Sleight, *Europhys. Lett.*, 1999, **46**, 661.
68 J. S. O. Evans, Z. Hu, J. D. Jorgensen, D. N. Argyriou, S. Short and A. W. Sleight, *Science*, 1997, **275**, 61.
69 J. D. Jorgensen, Z. Hu, S. Teslic, D. N. Argyriou, S. Short, J. S. O. Evans and A. W. Sleight, *Phys. Rev. B*, 1999, **59**, 215.
70 Z. Hu, J. D. Jorgensen, S. Teslic, S. Short, D. N. Argyriou, J. S. O. Evans and A. W. Sleight, *Physica B*, 1997, **241**, 370.
71 J. S. O. Evans, J. Jorgensen, R. M. Ibberson, W. I. F. David and A. W. Sleight, *Phys. Rev. B*, 1999, submitted.
72 C. A. Perottoni and J. A. H. Da Jornada, *Science*, 1998, **280**, 886.
73 A. P. Wilkinson, C. Lind and S. Pattanaik, *Chem. Mater.*, 1999, **11**, 101.
74 C. Closmann, A. W. Sleight and J. C. Haygarth, *J. Solid State Chem.*, 1998, **139**, 424.
75 C. Lind, A. P. Wilkinson, Z. B. Hu, S. Short and J. D. Jorgensen, *Chem. Mater.*, 1998, **10**, 2335.
76 N. Khosrovani, V. Korthuis, A. W. Sleight and T. Vogt, *Inorg. Chem.*, 1996, **35**, 485.
77 N. Khosrovani, A. W. Sleight and T. Vogt, *J. Solid State Chem.*, 1997, **132**, 355.
78 V. Korthuis, N. Khosrovani, A. W. Sleight, N. Roberts, R. Dupree and W. W. Warren, *Chem. Mater.*, 1995, **7**, 412.
79 G. Peyronel, *Gazz. Chim. Ital.*, 1942, **72**, 83.
80 G. R. Levi and G. Peyronel, *Z. Kristallogr.*, 1935, **92**, 190.
81 H. Vollenke, A. Wittmann and H. Novotny, *Monatsh. Chem.*, 1963, **94**, 956.
82 R. W. G. Wyckoff, *Z. Kristallogr.*, 1925, **62**, 189.
83 J. S. O. Evans, J. C. Hanson and A. W. Sleight, *Acta Crystallogr.*, *Sect. B*, 1998, **54**, 705.
84 R. L. Withers, J. S. O. Evans, J. Hanson and A. W. Sleight, *J. Solid State Chem.*, 1998, **137**, 161.
85 D. K. Seo and M. H. Whangbo, *J. Solid State Chem.*, 1997, **129**, 160.
86 G. V. Gibbs, J. W. Downs and M. B. Boisen Jr., in *Silica Physical Behavior, Geochemistry and Materials Applications*, ed. P. J. Heaney, C. T. Prewitt and G. V. Gibbs, *Rev. Mineral.*, 1994, **24**, 331.
87 S. C. Abrahams, *J. Chem. Phys.*, 1966, **45**, 2745.
88 J. S. O. Evans, T. A. Mary and A. W. Sleight, *J. Solid State Chem.*, 1997, **133**, 580.
89 J. S. O. Evans, T. A. Mary and A. W. Sleight, *J. Solid State Chem.*, 1995, **120**, 101.
90 A. W. Sleight and L. H. Brixner, *J. Solid State Chem.*, 1973, **7**, 172.
91 P. M. Forster, A. Yokochi and A. W. Sleight, *J. Solid State Chem.*, 1998, **140**, 157.
92 P. M. Forster and A. W. Sleight, *J. Inorg. Mater.*, 1999, in the press.
93 S. Senbhagaraman, T. N. G. Row and A. M. Umarji, *J. Mater. Chem.*, 1993, **3**, 309.
94 I. Yamai, T. Ota and P. Jin, *J. Ceram. Soc. Jpn.* (*Jpn. Ed.*), 1988, **96**, 1019.
95 N. A. Dhas and K. C. Patil, *J. Mater. Chem.*, 1995, **5**, 1463.
96 D. K. Agrawal, C. Y. Huang and H. A. McKinstry, *Int. J. Thermophys.*, 1991, **12**, 697.
97 C. Y. Huang, D. K. Agrawal and H. A. McKinstry, *J. Mater. Sci.*, 1995, **30**, 3509.
98 E. Breval and D. K. Agrawal, *Br. Ceram. Trans. J.*, 1995, **94**, 27.
99 J. F. Cloer, D. K. Agrawal and H. A. McKinstry, *J. Mater. Sci. Lett.*, 1988, **7**, 422.
100 D. M. Liu and J. J. Brown, *Mater. Chem. Phys.*, 1993, **33**, 43.
101 P. Lightfoot, D. A. Woodcock, J. D. Jorgensen and S. Short, *Int. J. Inorg. Mater.*, 1999, **1**, 53.
102 G. E. Lenain, H. A. McKinstry, J. Alamo and D. K. Agrawal, *J. Mater. Sci.*, 1987, **22**, 17.
103 J. Alamo, *Solid State Ionics*, 1993, **63-5**, 547.
104 D. A. Woodcock, P. Lightfoot and C. Ritter, *Chem. Commun.*, 1998, 107.
105 A. Bieniok and K. D. Hammonds, *Microporous Mesoporous Mater.*, 1998, **25**, 193.
106 D. A. Woodcock, P. Lightfoot, P. A. Wright, L. A. Villaescusa, M. J. DiazCabanas and M. A. Camblor, *J. Mater. Chem.*, 1999, **9**, 349.
107 M. P. Attfield and A. W. Sleight, *Chem. Commun.*, 1998, 601.
108 M. P. Attfield and A. W. Sleight, *Chem. Mater.*, 1998, **10**, 2013.
109 P. Tschaufeser and S. C. Parker, *J. Phys. Chem.*, 1995, **99**, 10600.
110 D. J. Williams, D. E. Partin, F. J. Lincoln, J. Kouvetakis and M. O'Keeffe, *J. Solid State Chem.*, 1997, **134**, 164.

Paper 9/04297K